Electrochimica Acta 258 (2017) 1106–1114

Contents lists available at ScienceDirect

Electrochimica Acta

journal homepage: www.elsevier.com/locate/electacta

Solid polymer electrolytes incorporating cubic $Li_7La_3Zr_2O_{12}$ for all-solid-state lithium rechargeable batteries

Fei Chen [a, *], Dunjie Yang [a], Wenping Zha [a], Bodi Zhu [a], Yanhua Zhang [a], Junyang Li [a], Yuping Gu [a], Qiang Shen [a], Lianmeng Zhang [a], Donald R. Sadoway [b]

[a] State Key Lab of Advanced Technology for Materials Synthesis and Processing, Wuhan University of Technology, Wuhan 430070, China
[b] Department of Materials Science and Engineering, Massachusetts Institute of Technology, Cambridge 02179, MA, USA

ARTICLE INFO

Article history:
Received 24 June 2017
Received in revised form
21 November 2017
Accepted 21 November 2017
Available online 22 November 2017

Keywords:
Solid electrolytes
Polyethylene oxide (PEO)
$Li_7La_3Zr_2O_{12}$ (LLZO)
Ionic conductivity

ABSTRACT

The advantages of all-solid-state batteries in terms of high energy density and improved safety have accelerated the research into durable and reliable solid electrolytes and into scale up of their processing technology. High lithium-ion-conducting $Li_7La_3Zr_2O_{12}$ (LLZO) ceramic-based solid electrolytes have been intensively studied recently, but their widespread commercial deployment has been constrained due to their fragility and brittleness. In the present study, LLZO ceramic powders have been successfully incorporated into the polyethylene oxide (PEO) polymer by tape casting. The ionic conductivity of the PEO/LLZO composite electrolyte membranes is significantly enhanced at the optimal LLZO concentration of 7.5 wt.% at which the materials exhibits maximum ionic conductivity of 5.5×10^{-4} S·cm^{-1} at 30 °C. The ionic conductivity enhancement mechanism of the composite electrolyte is revealed by differential scanning calorimetry (DSC), which shows that the LLZO filler represses crystallinity in PEO. Furthermore, as evidence of the advantageous electrochemical properties of the composite electrolyte an all-solid-state battery of $LiFePO_4$/Li fabricated herein delivered a maximum discharge capacity of 150.1 mAh·g^{-1} at 0.1C, good cycling performance, and excellent rate capability under 60 °C.

1. Introduction

Recently, lithium-ion batteries with high energy density, high output voltage and long cycle life with low capacity fading have gained great commercial success as the leading power source for electric vehicles and modern energy storage systems [1–4]. However, some safety hazards, such as uncontrolled side chemical reactions, Li dendrite formation, leakage and internal short circuits for the use of organic liquid electrolytes in lithium rechargeable batteries remain unresolved. In contrast to liquid electrolytes, the use of solid electrolytes has been proposed as a radical solution to the above problems [4,5]. Various inorganic solid electrolytes have been investigated for their advantages such as high mechanical, thermal, chemical, and electrochemical stability [5–8]. In addition to the inorganic solid electrolytes, significant attention has also been paid to solid polymer electrolytes (SPEs) with enhanced mechanical strength, flame-resistance, attractive form factor, and acceptably low cost [3,9,10]. Their numerous advantages open up the opportunity for fabrication of high packing efficiency, flexible, and safe all-solid-state lithium batteries.

Various SPEs based on high molecular weight dielectric polymer hosts, particularly, polyethylene oxide (PEO) doped with Li salts have been found to be suitable electrolytes for all-solid-state lithium battery designs in a free-standing form without major modification of current battery fabrication processes [11,12]. However, the use of PEO-based membranes in batteries is severely impeded by the low room-temperature conductivity (10^{-6}~10^{-8} S·cm^{-1}) which is the result of inherently high degree of polymer crystallinity below the transition temperature (~60 °C) [13,14]. To develop SPEs with high ionic conductivity and good mechanical properties, Some approaches have been tried such as adding liquid plasticizer, aligning polymer chains, and doping with ceramic fillers [15–17]. Of these alternates, adding ceramic fillers is believed to be an effective solution for its remarkable improvement in ionic conductivity and simplified fabrication procedures. The increase of ionic conductivity in ceramic-filler-doped polymers has been ascribed to the highly conductive amorphous phase stabilized by the inorganic ceramic fillers (Al_2O_3, SiO_2, $BaTiO_3$, etc.) [18–20] as

* Corresponding author.
E-mail address: chenfei027@gmail.com (F. Chen).

https://doi.org/10.1016/j.electacta.2017.11.164
0013-4686/

well as to the decrease in glass transition temperature of the polymer.

Although dispersing inorganic fillers in a polymer matrix can hinder polymer crystallization, issues such as ionic conductivity at room temperature (~10^{-4} S·cm^{-1}), interface stability, and electrochemical windows still restrict practical application of SPEs in an all-solid-state battery [21–23]. Herein we propose, instead of using conventional ceramic fillers which have no Li-ion conductivity, the use of ceramic powders with high ionic conductivity. Y.R. Zhao et al. [24] has incorporated $Li_{10}GeP_2S_{12}$ (LGPS) into PEO and a solid polymer electrolyte with a maximum ionic conductivity of 1.21×10^{-3} S·cm^{-1} at 80 °C was obtained. The effect of tetragonal Li_3N on the PEO matrix has been studied by J.P. Cho et al. [25] which exhibited ionic conductivity of 1.4×10^{-4} S·cm^{-1} at 80 °C. However, the LGPS is sensitive to air which makes processing difficult. Also, Li_3N has poor chemical and thermal stability (<2.5 V versus Li^+/Li).

Recently, the garnet structure inorganic solid electrolyte, $Li_7La_3Zr_2O_{12}$ (LLZO), first reported by Murugan et al. [26] has attracted attention due to its chemical stability with a lithium metal electrode, high ionic conductivity (10^{-3} ~10^{-4} S·cm^{-1}) at room temperature, low cost, and wide potential window (>5 V vs. Li/Li^+) [27]. However, most studies about LLZO have been focused on pellet-type ion conductors and thin-film solid electrolytes [28,29] and only few studies tried to elucidate the electrode design when applying the solid electrolytes [30]. Therefore, in order to get impressive energy density with the current system, the process compatibility with the conventional electrode preparation should be considered when designing an all-solid-state battery. The concept of combining ceramic and polymer with suitable mechanical properties offers advantages in battery design [31]. Several studies have tried to incorporate LLZO into a polymer owing to the superior electrochemical stability of LLZO. J.H. Choi et al. have studied composite membranes consisting of a polyethylene oxide (PEO) matrix with tetragonal $Li_7La_3Zr_2O_{12}$ (LLZO), which exhibited a ionic conductivity of 4.42×10^{-4} S·cm^{-1} at 55 °C [32]. The evidence that Li^+ favors the pathway through the LLZO ceramic phase in the composite electrolyte has been provided by J. Zheng et al. [33]. Dispersing nano-scale particles of garnet in insulating PEO has also been investigated [23]. Nevertheless, the focus of these studies was the electrolyte itself, rather than on the electrochemical performance of the composite electrolyte in all-solid-state lithium rechargeable batteries.

Herein, we report on an excellent free-standing solid polymer composite membrane with high ionic conductivity and good flexibility thanks to the addition cubic of $Li_7La_3Zr_2O_{12}$ (LLZO) powder as ceramic filler into the PEO matrix by tape casting. The morphology, ionic conductivity and interfacial properties of SPE membrane were systematically investigated.

2. Experimental procedures

2.1. Materials

The cubic LLZO was synthesized by field assisted sintering technology (FAST). Li_2O (99.99%, Aladdin), La_2O_3 (99.99%, Sinopharm Chemical Reagent Co., Ltd., China), and ZrO_2 (99.9%, Guangdong Orient Zirconic Ind. Sci. & Tech. Co., Ltd., China) powders were ball milled using zirconia balls in 2-propanol for about 12 h. The molar ratio of Li, La, and Zr was controlled as 7:3:2, and 1.5 wt.% γ- Al_2O_3 (99%, Aladdin) was added as cubic phase stabilized additive [27]. Then the powders were dried in a vacuum oven at 80 °C for 6 h. Next, the powders were loosely filled into the graphite die which was loaded into the FAST system operated with a plasma active sintering system (ED-PASIII, Elenix Ltd, Japan) for sintering at the temperature range of 900 °C–1230 °C under a constant uniaxial pressure of 10 MPa with a holding time of 3 min. The entire sintering process was conducted under an atmosphere of Ar which also balanced the pressure to prevent the loss of lithium. Preparing cubic LLZO by FAST can greatly reduce the Li loss with the high sintering rates and at the same time density LLZO, which has a great advantage over conventional methods such as solid state reaction and solution based methods. After the sample cooled down to room temperature naturally then it was ground into powder and screened with 200-mesh sieves. PEO (Mw = 6×10^5 g/mol, Aladdin) and LiTFSI (99.9%, Aldrich) were both vacuum dried at 50 °C for 24 h before use.

2.2. Preparation of composite polymer membrane

The composite polymer electrolyte membrane was prepared by tape casting. The molar ratio of PEO/LiTFSI was fixed at 8:1 and dissolved in acetonitrile (ACN, Aldrich Co. Ltd). LLZO powder with different weight ratios (range from 2.5 wt.% to 10 wt.% with respect to the weight of the composite membrane) was added respectively. Each slurry was cast onto a Teflon plate (200 mm × 150 mm × 50 mm) with grooves (140 mm × 140 mm × 250 μm) and was dried in a vacuum oven at 60 °C for 24 h after stirring for 24 h. Then the composite SPE membranes were stored in an argon-filled glove box.

2.3. Characterization

The phase structure of the LLZO and composite solid polymer membrane was characterized by X-ray diffraction (XRD, Rigaku Ultima III) with Cu Kα radiation (λ = 1.54178 Å) over the range of 10–90° (2θ). The SEM images of the composite solid polymer membrane and the microstructure of the LLZO were obtained by filed-emission scanning electron microscopy (FESEM, FEI-Quanta-250). FT-IR analysis of polymer electrolytes was performed at using the Nicolet6700 in the wave region of 4000–400 cm^{-1} with a wavenumber resolution of 2 cm^{-1}at room temperature.

The ionic conductivity of the composite solid polymer membranes was determined as a function of temperature between 30 °C and 80 °C by an electrochemical work station (CHI660E, Shanghai Chenhua instrument Co., Ltd.) with a signal amplitude of 5 mV over the frequency range from 10^{-2} Hz–10^6 Hz. The composite solid polymer membranes were sandwiched between two symmetrical stainless steel blocking electrodes of diameter 16 mm. The ionic conductivity was calculated using the following equation:

$$\sigma = \frac{L}{R_b S} \quad (1)$$

where σ (S·cm^{-1}) is the ionic conductivity, the R_b (Ω) is value of the bulk resistance, L (cm) is the thickness of the composite solid polymer membrane, and S (cm^2) is the area of symmetrical electrode. And three batches of samples were measured respectively for the accuracy of the data.

In order to evaluate the thermal properties of the composite electrolytes, differential scanning calorimetry (DSC) measurements were conducted on a Perkin Elmer Diamond DSC instrument with an interval of 10 °C from 40 °C to 200 °C under N_2 atmosphere.

The linear sweep voltammetry (LSV) experiments were performed in a three-electrode cell with a scanning rate of 0.5 mV·s^{-1} at 60 °C from 2.5 V to 6 V (vs. Li^+/Li). The cell was fitted with a working electrode of stainless steel and metallic Li as the counter and reference electrodes to investigate the electrochemical stability window of the composite electrolytes.

The lithium-ion transference number (t_{Li^+}) of the composite

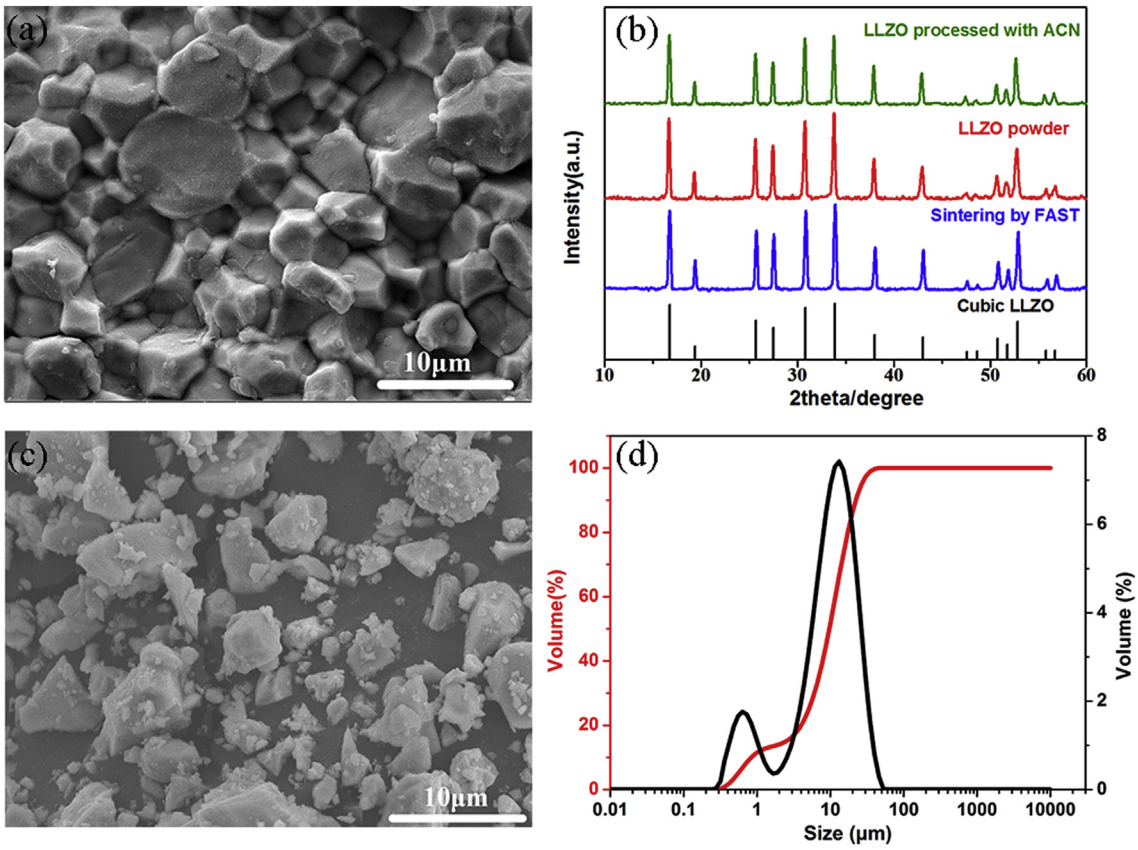

Fig. 1. (a) FESEM image of the LLZO pellet by FAST; (b) X-ray diffraction patterns of the LLZO pellet and LLZO powder; (c) FESEM image of the LLZO powder and (d) the particles size distribution of the LLZO powder.

electrolytes was measured at 60 °C in a symmetric Li/composite electrolyte/Li cell with a DC polarization voltage of 10 mV associated with the AC impedance measurement, and calculated following Eq. (2). The initial (I_0) and steady (I_{ss}) currents were obtained from a DC polarization test. R_0 and R_{ss} were obtained from the AC impedance measurement with the frequency between 10 MHz and 0.01 Hz representing the interface impedance before and after the test, respectively.

$$t_{Li^+} = \frac{I_{ss}(\Delta V - I_0 R_0)}{I_0(\Delta V - I_{ss} R_{ss})} \quad (2)$$

The electrochemical performance of all-solid-state batteries was tested on a Land charge/discharge instrument (Wuhan Rambo Testing Equipment Co., Ltd.) by assembling a 2025 coin-type cell with a $LiFePO_4$ cathode and a lithium metal anode. The cathode was made up of 75 wt.% $LiFePO_4$ powder, 20 wt.% Super-P and 5 wt.% composite electrolyte for improving the ion conduction of the cathode as well as acting as the binding material instead of PVDF which is commonly used in lithium batteries [34]. All of the materials above then were dissolved in acetonitrile (ACN, Aldrich Co. Ltd) and coated in aluminum foil. Then the cathode was dried at 100 °C under vacuum atmosphere for 48 h and pressed to ensure good contact with aluminum foil. The charge-discharge tests of the fabricated coin cell were conducted at different currents over the potential range of 2.8–4 V vs. Li/Li^+ at 60 °C.

3. Results and discussion

According to a previous report [26], there are two phases of LLZO: cubic and tetragonal. The bulk Li-ion conductivity for cubic LLZO used in this study is 10^{-3}~10^{-4} $S \cdot cm^{-1}$, which is suitable for battery applications, whereas the conductivity of tetragonal LLZO (~10^{-6} $S \cdot cm^{-1}$) makes it unsuitable [27]. In order to identify the microstructure and crystal size of the prepared LLZO, XRD patterns of the LLZO sintered by FAST and LLZO powder are shown in Fig. 1b. These results indicate that the synthesized LLZO powders are pure cubic phase. The results of the LLZO processed with ACN also indicate the stability of LLZO. Fig. 1a and c show SEM micrographs of the LLZO pellet and the LLZO powder after ball-milling. The particles have grown to a homogeneous size in the range of 10–15 μm. Additionally, the size distribution of the LLZO powder (Fig. 1d) indicates that the mean powder particle size is about 10 μm.

PEO is one of the semi-crystalline polymers. The amorphous phase within PEO structure provides activated chain segments, which aids ion mobility [35]. Most previous studies indicate that PEO crystallization is considered to adversely affect ion conductivity owing to the slowed polymer chain dynamics upon crystallization and the inactive chain segments [36]. Therefore, most reports have attempted to increase the percentage of the amorphous phase of PEO and to decrease the interaction between the Li ions and PEO chains in order to improve the Li ion conductivity. In the field of SPEs based on PEO, the addition of inorganic oxides and ceramic fillers such as Al_2O_3 and SiO_2 into the PEO matrix can improve the ionic conductivity because of the increase in amorphous phase of PEO and the attendant impeding of crystallization. In Fig. 2a, X-ray diffraction spectra of PEO/LLZO with different LLZO contents are shown, indicating its effect on the crystalline behavior of PEO. We see the appearance of characteristic diffraction peaks in

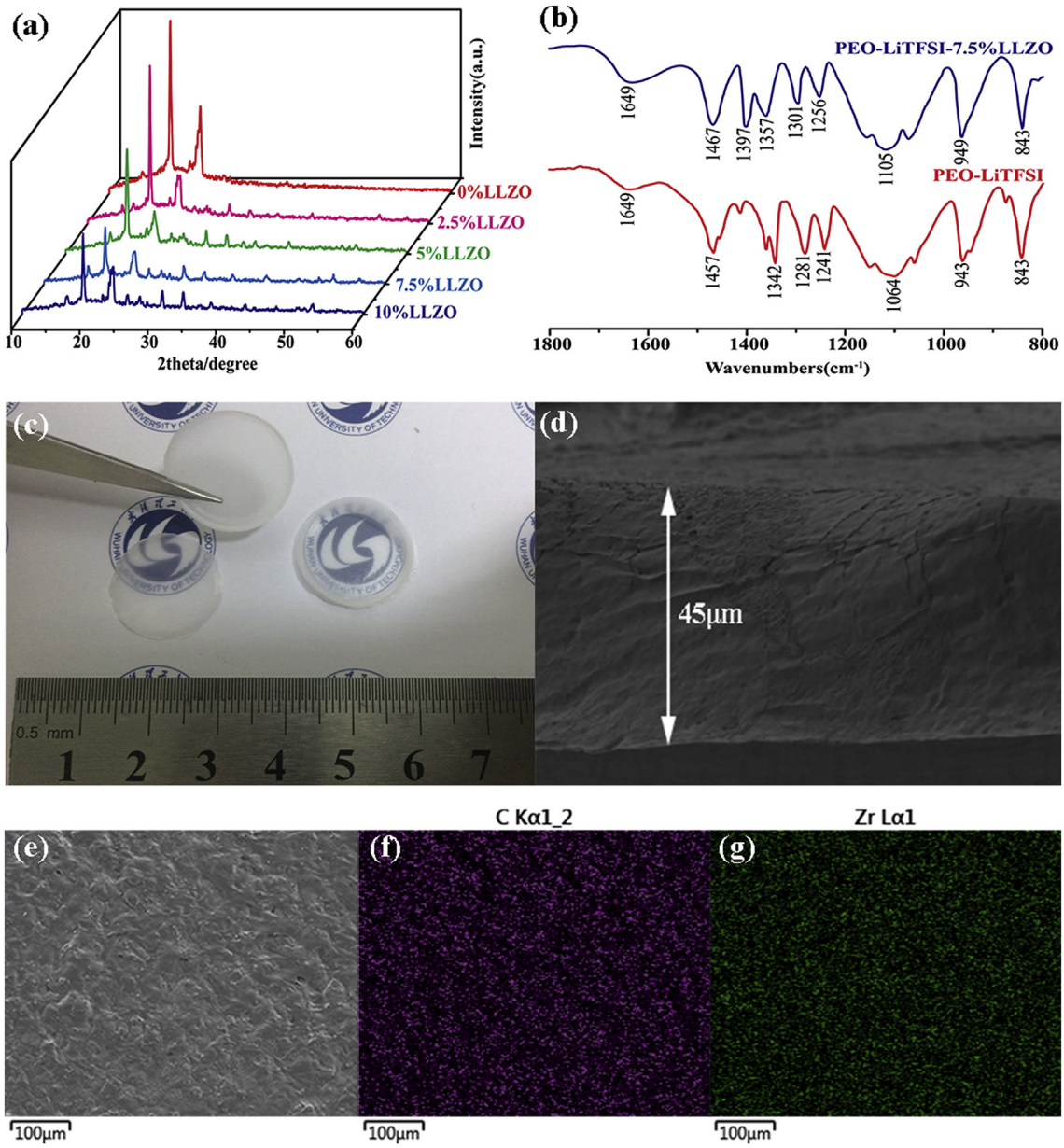

Fig. 2. (a) X-ray diffraction patterns of the pure PEO and the solid composite polymer electrolyte with various LLZO contents; (b) FTIR spectra of PEO-LiTFSI and PEO-LiTFSI-7.5% LLZO; (c) the image of the composite electrolyte; (d) the cross section of the SPE; and (e) SEM images of the SPEs and EDS maps of (f) C and (g) Zr in the sample marked.

the range of $2\theta = 19°–23°$. A drop on peak intensity can be observed on PEO/LLZO composite electrolyte at various LLZO contents, indicating that LLZO can reduce the crystallinity of PEO matrix and increase amorphous phase. As the incorporation content of LLZO into the PEO matrix increased, further decreases in peak intensity are detected. This phenomenon can be explained by the disruptive effect of the LLZO particles on the ordered arrangement of the polymer side chains, and also as a result of the increase in the percentage of the amorphous phase. To confirm the addition of LLZO has an effect on the structure of PEO matrix structure, FTIR spectra of PEO-LiTFSI and PEO-LiTFSI-7.5%LLZO composite electrolyte are measured and shown in Fig. 2b, Apparently, there are two main differences in the spectrum of the PEO-LiTFSI-7.5%LLZO electrolyte in comparison with that of the PEO-LiTFSI electrolyte. The first one is that the wave number increased to 1105 cm^{-1} from 1064 cm^{-1} that is characteristic of C–O–C stretching mode when adding LLZO into the PEO-LiTFSI electrolyte. Suggesting the interaction between the –OH groups on the surface of LLZO particles and the ether oxygen group in PEO has weakened the complexation of Li^+ with ether oxygen groups. The second one is the changes of adsorption peaks (943, 1241 and 1281 cm^{-1} shift to 949, 1256 and 1301 cm^{-1}) corresponding to the CH_2 bending vibration mode [37] and lowering the intensity of adsorption, it also indicated the attenuation of the complexation between ether oxygen groups and Li^+ [38]. Fig. 2c shows the prepared composite electrolyte to be translucent and the thickness to be 45 μm as shown in Fig. 2d which can be easily adjusted by the amount of precursor solution. Meanwhile, the SEM image of the solid composite polymer electrolyte membrane with 7.5 wt.% cubic LLZO prepared by tape casting is shown in Fig. 2e. We can see from the surface of the

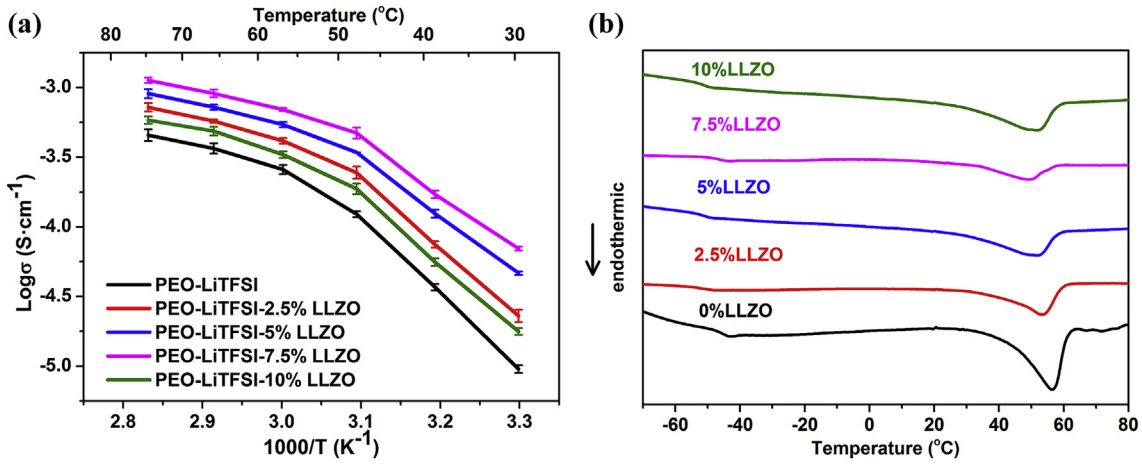

Fig. 3. (a) Arrhenius plots for the ionic conductivities of SPE samples. (b) Differential scanning calorimetry curves of the membranes with various LLZO contents.

Table 1
The values of the glass transition temperature (T_g), the crystalline melting temperature (T_m) and the heat enthalpy (ΔH_m) from DSC measurement and $\Delta\chi_c$ of electrolytes.

Electrolytes	T_g	T_m	ΔH_m	χ_c
PEO-LiTFSI	−46.56	56.44	109.2749	53.83%
PEO-LiTFSI-2.5%LLZO	−46.79	56.21	51.5011	25.37%
PEO-LiTFSI-5%LLZO	−47.34	53.27	46.3043	22.81%
PEO-LiTFSI-7.5%LLZO	−47.63	52.78	43.9089	21.63%
PEO-LiTFSI-10%LLZO	−47.90	54.07	59.1948	29.16%

composite electrolyte no voids could be detected. The EDS mapping images of the elements C, Zr on the surface of the composite solid electrolyte are also shown in Fig. 2e and g. The elemental mappings indicate that the cubic LLZO particles are dispersed homogeneously in the PEO matrix.

High ionic conductivity of the PEO/LLZO composite electrolyte at room temperature is prerequisite for real application of solid-state batteries. Arrhenius plots of ionic conductivity with temperature varied from 30 °C to 80 °C for analyzing the mechanism of ionic conduction in the PEO/LLZO composite electrolyte are shown in Fig. 3a. It is evident that the composite membrane doped with 7.5 wt.% cubic LLZO possesses the maximum ionic conductivity of 5.5×10^{-4} S·cm^{-1} at room temperature. With the further increase of the cubic LLZO content, the ionic conductivity is decreased. The concept as discussed above that inhibition in crystallization of PEO results in increase in the ionic conductivity can explain these phenomena. Therefore, incorporating into the PEO matrix the cubic LLZO as inorganic ionic conductor with high lithium ion conductivity at room temperature compared to the inert ceramic filler such as Al_2O_3 and SiO_2 can have a synergetic effect on the Li ionic conductivity. When the Li ions transfer between PEO side chains in the amorphous phase, the cubic LLZO can participate in ion transport by providing for enhanced free lithium ion concentrations, lithium ion surface conduction, anion attraction, and a lithium ion source [5].

The activation energies of the various membranes were calculated by using the following equation:

$$\sigma = A\exp\left(\frac{-E_a}{kT}\right) \quad (3)$$

where σ is the ionic conductivity, A is the pre-exponential constant, E_a is the activation energy for lithium ion conduction, k is the Boltzmann constant, and T is the absolute temperature. It is clearly revealed in Fig. 3a that the composite electrolyte has distinctive ionic conductivities in the high temperature region (50–80 °C) and the low temperature region (30–50 °C), which is consistent with previous results when PEO was combined with other active inorganic fillers such as $Li_{10}GeP_2S_{12}$ (LGPS) [24]. Obviously, the curve has an inflection point around 50 °C which we attribute to the crystallinity of PEO at higher temperature, it is amorphous; at lower temperature crystallinity sets in. The activation energies of the composite membranes were calculated to be in the range 140–160 kJ·mol^{-1} in the lower temperature region (30–50 °C); in contrast, in the higher temperature region (50–80 °C) the activation energies are in the range 30–60 kJ·mol^{-1}. When the composite electrolytes are at high temperature, which is approximately the melting point of PEO, the PEO/LLZO composite electrolyte is in a melted state which benefits ion transport. At low temperature, the PEO becomes solid and conductivity decreases rapidly as ion transport in the PEO matrix turns into a slow process of breaking/forming lithium-oxygen (Li–O) bonds involving the ether oxygen atoms on a segmental PEO chain coordinated with lithium ions [39]. The segmental motion of the chain becomes slow when the PEO solidifies at low temperature; at the same time the solid PEO inhibits the transport of Li ions between LLZO particles. Likewise,

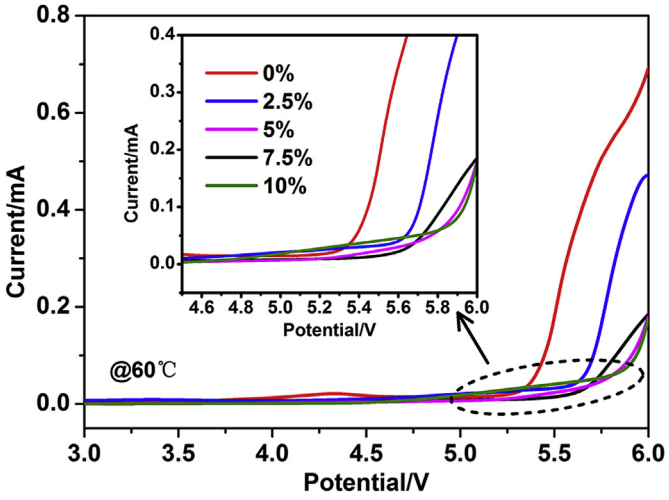

Fig. 4. The electrochemical stability window of LSV curves at 60 °C.

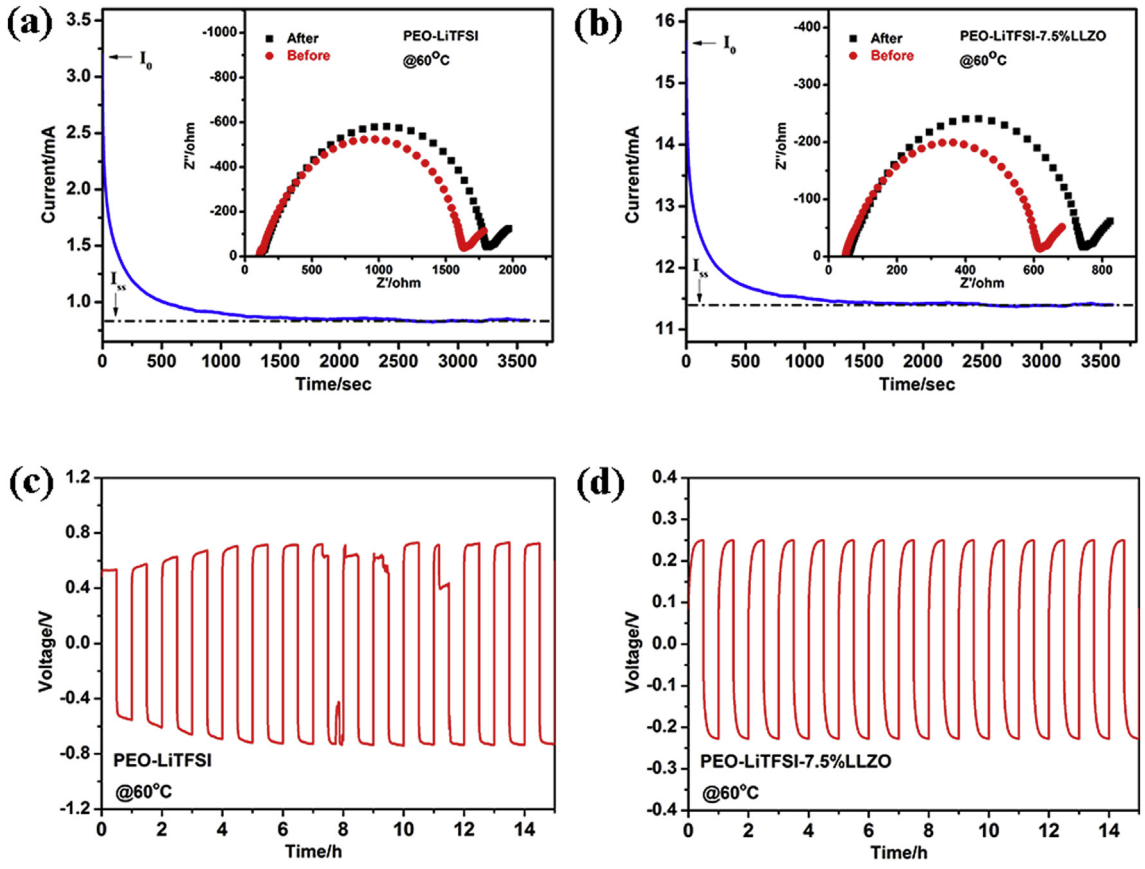

Fig. 5. The measurement of impedance spectra and DC polarization at 60 °C for (a) PEO-based electrolyte and (b) composite electrolyte and voltage profiles of the symmetrical Li/electrolyte/Li cells with (c) PEO-based electrolyte and (d) composite electrolytes at a current density of 0.2 mAh cm^{-2} at 60 °C.

Table 2
Measured values for the parameters in Eq. (2) and the corresponding calculated values of lithium ion transference numbers (t_{Li^+}) at 60 °C.

Electrolytes	I_0/μA	I_{ss}/μA	R_0/Ω	R_{ss}/Ω	ΔV/mV	t_{Li^+}
PEO-LiTFSI	3	0.8	1635	1800	10	0.159
PEO-LiTFSI-7.5%LLZO	15.7	11.43	610	745	10	0.207

the high content cubic LLZO within the PEO/LLZO composite electrolyte dilutes the PEO, which plays an important role in the connection between LLZO particles. Therefore, the conductivity is almost the same as pure PEO electrolyte.

In order to determine the influence of the LLZO powder on the crystallinity of the PEO matrix, the thermal behavior of the composite membranes was investigated by differential scanning calorimetry (DSC) which is illustrated in Fig. 3b. All curves show one defined endothermic peak in the temperature range between −80 °C and 80 °C. Also shown is the shift to lower temperatures of the endothermic reaction with increase in the LLZO content. Meanwhile, the glass transition temperature (T_g), the crystalline melting temperature (T_m), and the heat enthalpy (ΔH_m) of the composite electrolyte have changed by the addition of LLZO. The values above are summarized in Table 1.

The crystallinities (χ_c) of the composite polymer electrolytes are calculated by Eq. (4), where χ_c shows the relative percentage of crystallinity for pure PEO electrolyte, ΔH_m is the melting enthalpy of electrolyte, and ΔH_{peo} is the value of ΔH_m for PEO having completely crystallized (203 $J \cdot g^{-1}$) [40], and f_{peo} is the PEO mass percentage in the composite electrolyte.

$$\chi_c = \frac{\Delta H_m}{\Delta H_{peo} f_{peo}} \times 100\% \quad (4)$$

As shown in Fig. 3b the T_g and T_m decrease with incorporation of LLZO, which, in turn, leads to an increase in the fraction of the amorphous phase. Lithium ion mobility in the non-crystalline phase is higher than that in the crystalline phase. In addition, the χ_c of the composite electrolyte decreased from 53.83% to 21.63% as the LLZO content increased from 0% to 7.5% which is in accordance with the DSC data. It suggests that the addition of LLZO can effectively inhibit PEO's crystallization. With the increase of LLZO content, the crystallinity content is increased, which is ascribed to the fact that more and more excessive LLZO particles are difficult to disperse in PEO matrix and easy to form clusters. This makes the LLZO act as an insulator to blocks conducting pathways as well as improving the crystallinity of the LLZO/PEO composite.

An electrolyte with a wide electrochemical window is key to developing high-energy-density lithium-ion batteries. By linear sweep voltammetry (LSV) the electrochemical stability of the composite electrolytes was evaluated at 60 °C. The electrochemical window of LSV curves is shown in Fig. 4. In the PEO-only electrolyte, there is a peak in the anodic current near the potential of 4.3 V vs. Li/Li^+. This is mainly due to the Li^+ in lithium salt breakdown from the PEO. Another peak occurs at 5.0 V vs. Li/Li^+ while the composite electrolyte has a peak beyond 5.7 V vs. Li/Li^+ which is the decomposition voltage for electrolyte due to oxidation. The results also indicate that the LLZO incorporation into the PEO matrix results in better oxidation stability than that of the PEO-only electrolyte. This may arise from the high potential of LLZO [27] and

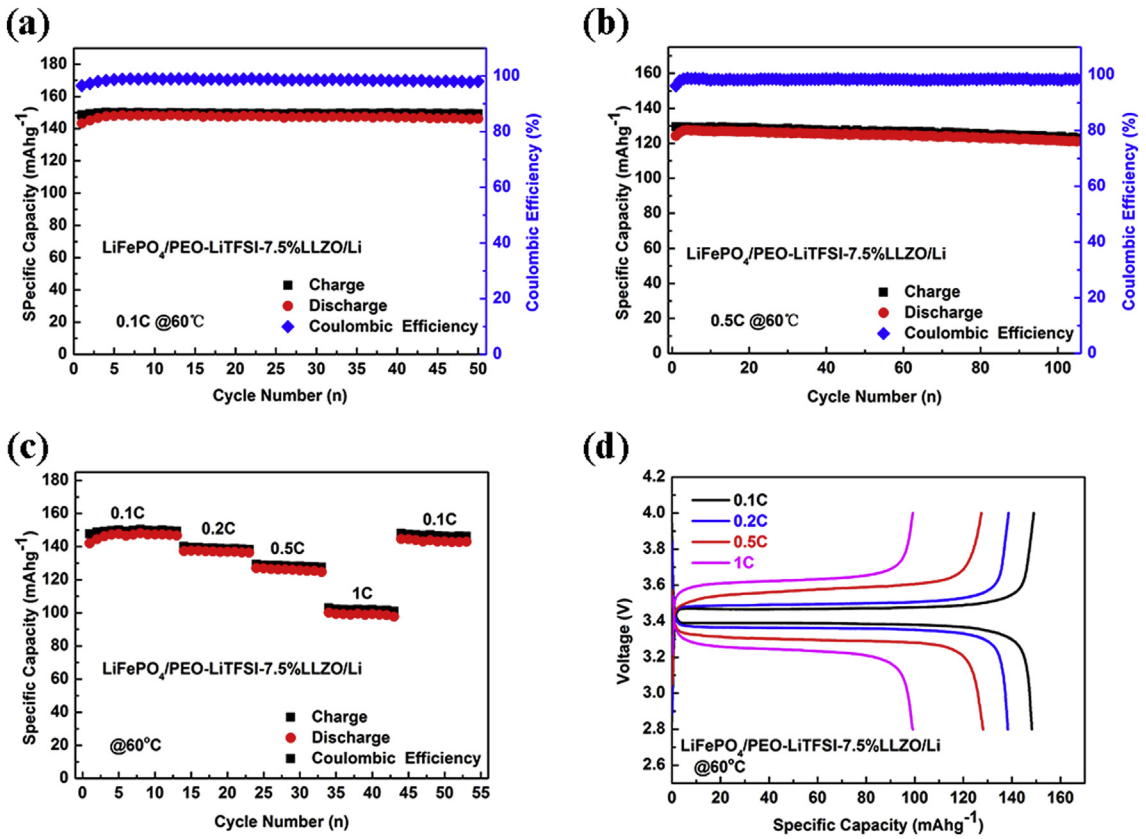

Fig. 6. The cycling performance of all-solid-state battery $LiFePO_4$/PEO-LiTFSI-7.5%LLZO/Li at (a) 0.1 C, (b) 0.5 C under 60 °C; (c) the rate performance at different rates (0.1 C, 0.2 C, 0.5C, and 1 C) and (d) the initial charge and discharge curves.

strong Lewis acid-base interaction between electrolyte ion species and the surface chemical groups of LLZO fillers which can enhance salt dissociation and stabilize the anions [41]. These results reveal that the composite electrolyte can be safely deployed in an all-solid-state battery using $LiFePO_4$ as the cathode which can cycle in the voltage range of 2.5–4.0 V.

Additionally, the lithium ion transference number (t_{Li^+}) had been determined by combining the measurements of impedance spectra and DC polarization at 60 °C. Results are shown in Fig. 5 and are summarized in Table 2 for both pure PEO and the composite electrolytes with 7.5 wt.% LLZO content. The value of t_{Li^+} for the composite electrolytes with 7.5 wt.% LLZO content is 0.207 and 0.159 for the PEO-only electrolyte. This enhancement could be explained by the fact that LLZO is an active lithium ion conductor in which the transport number is unity. Consequently, the incorporation of LLZO powder as inorganic filler in the PEO matrix not only improves the ionic conductivity but also achieved a positive effect on the electrochemical window and lithium ion transference number. The combination of these advantageous changes in properties make this a promising electrolyte for application to next-generation all-solid-state batteries. The interfacial behavior between a lithium electrode and the solid electrolyte also has been investigated with the symmetrical cell at a current density of 0.2 $mAh \cdot cm^{-2}$ under 60 °C. As shown in Fig. 5c and d, the cell with PEO-only solid polymer electrolyte exhibits instability with some short circuiting during operation. This mainly comes from the formation of lithium dendrites and poor electrochemical properties of pure PEO. Nevertheless, when the solid electrolyte is replaced by the composite electrolyte the cells are much more stable and exhibit superior voltage profiles. These results indicate that inorganic LLZO particles in the PEO matrix can reinforce electrochemical stability and ionic conductivity of SPEs and establish stable interfaces with a lithium metal anode.

In order to explore the application of the composite electrolyte, all-solid-state lithium batteries were fabricated with a Li negative electrode and a $LiFePO_4$ positive electrode and fitted with a composite electrolyte with 7.5 wt.%. LLZO content (short for PEO-LiTFSI-7.5%LLZO). The discharge capacity, cycling, and rate performance were measured. As illustrated in Fig. 6a, when the all-solid-state batteries were run under 0.1C, the discharge specific capacity is improved from 148.6 $mAh \cdot g^{-1}$ to the maximum 150.1 $mAh \cdot g^{-1}$ after 3 cycles; then the discharge specific capacity maintains 149.5 $mAh \cdot g^{-1}$ after 50 cycles, with 93.2% of the maximum specific capacity retained during the whole cycling process. The columbic efficiency held around 98.9%. The specific capacity of batteries increases rapidly during the initial several cycles which is ascribed to the activation process and the interfacial conditioning between the lithium electrode and the solid electrolyte [42]. To better illustrate the stability of the composite electrolyte, the all-solid-state batteries also performed at high rate (0.5C), the cycling performance shown in Fig. 6b. After the active process, the discharge specific capacity slightly decreases, and after 100 cycles, the discharge specific capacity is above 121 $mAh \cdot g^{-1}$. Capacity is 89% retained. This indicates that all-solid-state batteries have excellent cycling performance. Fig. 6c shows the cycling and rate performance of the Li/PEO-LiTFSI-7.5%LLZO/$LiFePO_4$ all-solid-state battery with the rate range from 0.1 C to 1 C with every 10 cycles. Before the cycling test, the cell was activated by 5 cycles at low current density (0.1 C). It is clearly seen that the specific capacity exhibits 100.2 $mAh \cdot g^{-1}$ at 1 C and the capacity could be quickly recovered when the rate

returns to 0.1 C. This is evidence of good rate stability of an all-solid-state battery fitted with the composite electrolyte.

The initial charge and discharge curves from 0.1 C to 1 C at 60 °C are shown in Fig. 6d. The first discharge specific capacities of the Li/PEO-LiTFSI-7.5%LLZO/$LiFePO_4$ all-solid-state battery at 0.1 C, 0.2 C, 0.5 C, and 1 C are 150.1, 138.6, 127.5, and 100.2 $mAh \cdot g^{-1}$, respectively. Meanwhile, the cell presents two charge voltage plateaus at around 3.38 and 3.45 V when operating at 0.1 C, corresponding to the Fe^{2+}/Fe^{3+} redox couple reaction on the cathode. The low polarization voltage in an all-solid-state battery is attributed to the small electrolyte resistance and small interfacial resistance on both anode and cathode as discussed above [43].

4. Conclusions

Solid composite polymer electrolyte membranes composed of PEO and 2.5–10 wt.% cubic LLZO have been synthesized by tape casting. We found that the as-prepared composite polymer electrolyte membranes exhibit enhanced ionic conductivity compared to that of the PEO-only electrolyte membranes and cubic LLZO electrolyte. Impedance spectroscopy revealed that the composite electrolyte membrane containing 7.5% cubic LLZO exhibited the highest ionic conductivity (5.5×10^{-4} $S \cdot cm^{-1}$ at 30 °C) thanks to the synergetic effect of the cubic LLZO. The phase transition behaviors of the composite polymer electrolytes were characterized by DSC, which show that the cubic LLZO particles in PEO matrix increase effectively the percentage of the amorphous phase of PEO. The results of the lithium ion transference numbers illustrate that the solid composite electrolyte can promote the lithium ion transfer (the lithium ion transference numbers improved from 0.159 to 0.207). The LSV results showed that the electrochemical stability of the composite electrolyte is improved to 5.7 vs. Li/Li^+ compared with the PEO-only electrolyte. Finally, the all-solid-state lithium battery Li/PEO-LiTFSI-7.5%LLZO/$LiFePO_4$ delivers a high initial discharge capacity of 150.1 $mAh \cdot g^{-1}$ at 0.1C and 93.2% of the maximum specific capacity retained after 50 cycles. When the cell was run at high rate (0.5C), the specific capacity is 127.5 $mAh \cdot g^{-1}$. Meanwhile, it also exhibits good cycling and rate performance at 60 °C. The excellent electrochemical performance results from the composite cathode and solid electrolyte, in which the LLZO filler both improve the ion conductivity as an active ion conductor and improve the electrochemical stability of the PEO matrix. The composite electrolyte herein is attractive as a key component for next-generation all-solid-state lithium rechargeable batteries.

Acknowledgments

This work is financially supported by the National Natural Science Foundation of China (No. 51472188, and 51521001), Natural Research Funds of Hubei Province (No. 2016CFB583), Fundamental Research Funds for the Central Universities in China, State Key Laboratory of Advanced Electromagnetic Engineering and Technology (Huazhong University of Science and Technology), National Key Research and Development Program of China (NO. 2017YFB0310400) and the “111” project (No. B13035).

References

[1] M. Armand, J.M. Tarascon, Building better batteries, Nature 451 (2008) 652–657.
[2] J.W. Fergus, Recent developments in cathode materials for lithium ion batteries, J. Power Sources 195 (2010) 939–954.
[3] R. Bouchet, S. Maria, R. Meziane, A. Aboulaich, L. Lienafa, J.P. Bonnet, T.N. Phan, D. Bertin, D. Gigmes, D. Devaux, R. Denoyel, M. Armand, Single-ion BAB triblock copolymers as highly efficient electrolytes for lithium-metal batteries, Nat. Mater. 12 (2013) 452–457.
[4] P.P. Soo, B. Huang, Y.I. Jang, Y.M. Chiang, D.R. Sadoway, A.M. Mayes, Rubbery block copolymer electrolytes for solid-state rechargeable lithium batteries, J. Electrochem. Soc. 146 (1999) 32–37.
[5] N. Kamaya, K. Homma, Y. Yamakawa, M. Hirayama, R. Kanno, M. Yonemura, T. Kamiyama, Y. Kato, S. Hama, K. Kawamoto, A lithium superionic conductor, Nat. Mater. 10 (2011) 682.
[6] K. Xu, Electrolytes and interphases in Li-Ion batteries and beyond, Chem. Rev. 114 (2014) 11503–11618.
[7] P.E. Trapa, Y.Y. Won, S.C. Mui, E.A. Olivetti, B. Huang, D.R. Sadoway, A.M. Mayes, S. Dallek, Rubbery graft copolymer electrolytes for solid-state, thin-film lithium batteries, J. Electrochem. Soc. 152 (2005) A1–A5.
[8] M. Kurian, M.E. Galvin, P.E. Trapa, D.R. Sadoway, A.M. Mayes, Single-ion conducting polymer–silicate nanocomposite electrolytes for lithium battery applications, Electrochim. Acta 50 (2005) 2125–2134.
[9] G.M. Stone, S.A. Mullin, A.A. Teran, J.D.T. Hallinan, A.M. Minor, A. Hexemer, N.P. Balsara, Resolution of the modulus versus adhesion dilemma in solid polymer electrolytes for rechargeable lithium metal batteries, J. Electrochem. Soc. 159 (2012).
[10] K.J. Harry, D.T. Hallinan, D.Y. Parkinson, A.A. Macdowell, N.P. Balsara, Detection of subsurface structures underneath dendrites formed on cycled lithium metal electrodes, Nat. Mater. 13 (2014) 69–73.
[11] B. Scrosati, J. Garche, Lithium batteries: status, prospects and future, J. Power Sources 195 (2010) 2419–2430.
[12] F.M. Gray, T.G. House, RSC Materials Monographs, Royal Society of Chemistry, 1997.
[13] S.K. Fullertonshirey, J.K. Maranas, Effect of $LiClO_4$ on the structure and mobility of PEO-based solid polymer electrolytes, Macromolecules 42 (2009) 2142–2156.
[14] J.G. Kim, B. Son, S. Mukherjee, N. Schuppert, A. Bates, O. Kwon, M.J. Choi, H.Y. Chung, S. Park, A review of lithium and non-lithium based solid state batteries, J. Power Sources 282 (2015) 299–322.
[15] Q. Wang, W.L. Song, L.Z. Fan, Q. Shi, Effect of alumina on triethylene glycol diacetate-2-propenoic acid butyl ester composite polymer electrolytes for flexible lithium ion batteries, J. Power Sources 279 (2015) 405–412.
[16] L.Y. Yang, D.X. Wei, M. Xu, Y.F. Yao, Q. Chen, Transferring lithium ions in nanochannels: a PEO/Li^+ solid polymer electrolyte design, Angew. Chem. 126 (2014) 3705–3709.
[17] C. Tang, K. Hackenberg, Q. Fu, P.M. Ajayan, H. Ardebili, High ion conducting polymer nanocomposite electrolytes using hybrid nanofillers, Nano Lett. 12 (2012) 1152–1156.
[18] D. Lin, W. Liu, Y. Liu, H.R. Lee, P.C. Hsu, K. Liu, Y. Cui, High ionic conductivity of composite solid polymer electrolyte via in situ synthesis of monodispersed SiO_2 nanospheres in poly(ethylene oxide), Nano Lett. 16 (2016) 459.
[19] Y. Liao, C. Sun, S. Hu, W. Li, Anti-thermal shrinkage nanoparticles/polymer and ionic liquid based gel polymer electrolyte for lithium ion battery, Electrochim. Acta 89 (2013) 461–468.
[20] S. Ishibe, K. Anzai, N. Jin, Y. Konosu, M. Ashizawa, H. Matsumoto, Y. Tominaga, Ion-conductive and mechanical properties of polyether/silica thin fiber composite electrolytes, React. Funct. Polym. 81 (2014) 40–44.
[21] W. Wang, E. Yi, A.J. Fici, R.M. Laine, J. Kieffer, Lithium ion conducting poly(-ethylene oxide)-based solid electrolytes containing active or passive ceramic nanoparticles, J. Phys. Chem. C 121 (2017) 2563–2573.
[22] W. Liu, N. Liu, J. Sun, P.C. Hsu, Y. Li, H.W. Lee, Y. Cui, Ionic conductivity enhancement of polymer electrolytes with ceramic nanowire fillers, Nano Lett. 15 (2015) 2740–2745.
[23] J. Zhang, N. Zhao, M. Zhang, Y. Li, P.K. Chu, X. Guo, Z. Di, X. Wang, H. Li, Flexible and ion-conducting membrane electrolytes for solid-state lithium batteries: dispersion of garnet nanoparticles in insulating polyethylene oxide, Nano Energy 28 (2016) 447–454.
[24] Y. Zhao, C. Wu, G. Peng, X. Chen, X. Yao, Y. Bai, F. Wu, S. Chen, X. Xu, A new solid polymer electrolyte incorporating $Li_{10}GeP_2S_{12}$ into a polyethylene oxide matrix for all-solid-state lithium batteries, J. Power Sources 301 (2016) 47–53.
[25] A. Manuel Stephan, K.S. Nahm, Review on composite polymer electrolytes for lithium batteries, Polymer 47 (2006) 5952–5964.
[26] R. Murugan, V. Thangadurai, W. Weppner, Fast lithium ion conduction in garnet-type Li(7)La(3)Zr(2)O(12), Angew. Chem. 46 (2007) 7778–7781.
[27] Y. Zhang, F. Chen, R. Tu, Q. Shen, L. Zhang, Field assisted sintering of dense Al-substituted cubic phase $Li_7La_3Zr_2O_{12}$ solid electrolytes, J. Power Sources 268 (2014) 960–964.
[28] E. Yi, W. Wang, J. Kieffer, R.M. Laine, Flame made nanoparticles permit processing of dense, flexible, Li+conducting ceramic electrolyte thin films of cubic-$Li_7La_3Zr_2O_{12}$(c-LLZO), J. Mater. Chem. A 4 (2016) 12947–12954.
[29] E. Yi, W. Wang, J. Kieffer, R.M. Laine, Key parameters governing the densification of cubic- $Li_7La_3Zr_2O_{12}$ Li^+ conductors, J. Power Sources 352 (2017) 156–164.
[30] K. Fu, Y. Gong, G.T. Hitz, D.W. McOwen, Y. Li, S. Xu, Y. Wen, L. Zhang, C. Wang, G. Pastel, J. Dai, B. Liu, H. Xie, Y. Yao, E.D. Wachsman, L. Hu, Three-dimensional bilayer garnet solid electrolyte based high energy density lithium metal–sulfur batteries, Energy Environ. Sci. 10 (2017) 1568–1575.
[31] S. Skaarup, K. West, B. Zachau-Christiansen, Mixed phase solid electrolytes, Solid State Ion. s28–30 (1988) 975–978.
[32] J.-H. Choi, C.-H. Lee, J.-H. Yu, C.-H. Doh, S.-M. Lee, Enhancement of ionic conductivity of composite membranes for all-solid-state lithium rechargeable batteries incorporating tetragonal $Li_7La_3Zr_2O_{12}$ into a polyethylene oxide matrix, J. Power Sources 274 (2015) 458–463.

[33] J. Zheng, M. Tang, Y.Y. Hu, Lithium ion pathway within $Li_7La_3Zr_2O_{12}$-Polyethylene oxide composite electrolytes, Angew. Chem. 128 (2016) 12726–12730.
[34] Q. Hu, S. Osswald, R. Daniel, Y. Zhu, S. Wesel, L. Ortiz, D.R. Sadoway, Graft copolymer-based lithium-ion battery for high-temperature operation, J. Power Sources 196 (2011) 5604–5610.
[35] P. Johansson, First principles modelling of amorphous polymer electrolytes: Li^+–PEO, Li^+–PEI, and Li $^+$–PES complexes, Polymer 42 (2001) 4367–4373.
[36] S. Cheng, D.M. Smith, C.Y. Li, How does nanoscale crystalline structure affect ion transport in solid polymer electrolytes? Macromolecules 43 (2014) 3978–3986.
[37] S. Ramesh, F.Y. Tai, C.J. Shen, Conductivity and FTIR studies on PEO–LiX [X: CF_3SO^{3-}, SO_4^{2-}] polymer electrolytes, Spectrochim. Acta Part A Mol. Biomol. Spectrosc. 69 (2008) 670–675.
[38] D. Saikia, H.Y. Wu, Y.C. Pan, C.C. Liao, C.F. Chen, G.T.K. Fey, H.M. Kao, A highly conductive organic–inorganic hybrid electrolyte based on co-condensation of di-ureasil and ethylene glycol-containing alkoxysilane, Electrochim. Acta 54 (2009) 7156–7166.
[39] Z. Xue, D. He, X. Xie, Poly(ethylene oxide)-based electrolytes for lithium-ion batteries, J. Mater. Chem. A 3 (2015) 19218–19253.
[40] X.L. Wu, S. Xin, H.H. Seo, J. Kim, Y.G. Guo, J.S. Lee, Enhanced Li^+ conductivity in PEO–LiBOB polymer electrolytes by using succinonitrile as a plasticizer, Solid State Ion. 186 (2011) 1–6.
[41] J. Zhou, P.S. Fedkiw, Ionic conductivity of composite electrolytes based on oligo(ethylene oxide) and fumed oxides, Solid State Ion. 166 (2004) 275–293.
[42] B. Chen, Z. Huang, X. Chen, Y. Zhao, Q. Xu, P. Long, S. Chen, X. Xu, A new composite solid electrolyte PEO/$Li_{10}GeP_2S_{12}$/SN for all-solid-state lithium battery, Electrochim. Acta 210 (2016) 905–914.
[43] Q. Lu, J. Fang, J. Yang, G. Yan, S. Liu, J. Wang, A novel solid composite polymer electrolyte based on poly(ethylene oxide) segmented polysulfone copolymers for rechargeable lithium batteries, J. Membr. Sci. s425–426 (2013) 105–112.